Article

JOURNAL OF COMPOSITE MATERIALS

Journal of Composite Materials
45(24) 2523–2536

DOI: 10.1177/0021998311401103
jcm.sagepub.com
SAGE

Two higher order Zig-Zag theories for the accurate analysis of bending, vibration and buckling response of laminated plates by radial basis functions collocation and a unified formulation

A.J.M. Ferreira[1], C.M.C. Roque[2], E. Carrera[3], M. Cinefra[3] and O. Polit[4]

Abstract

In this article, we combine the Carrera's Unified Formulation, CUF (Carrera E. Theories and Finite elements for multilayered plates and shells: A unified compact formulation with numerical assessment and benchmarking. *Arch. Comput. Methods Eng.*, 2003; **10**: 215–297.) and a radial basis function collocation technique for predicting the static deformations, free vibrations and buckling behavior of thin and thick cross-ply laminated plates. We develop by the CUF two Zig-Zag theories according to Murakami's Zig-Zag function. Both theories account for through-the-thickness deformations, allowing the analysis of thick plates. The accuracy and efficiency of this collocation technique for static, vibration, and buckling problems are demonstrated through numerical examples.

Keywords

laminated plates, collocation, radial basis functions, unified formulation, plates and shells, composites

Introduction

Multilayered structures show a piece-wise continuous displacement field in the thickness plate/shell direction. This change in slope between two adjacent layers, that are considered to be perfectly bonded together, is known as the Zig-Zag (ZZ) effect (Figure 1). The different transverse (both shear and normal components) deformability of the layers is the source of the ZZ effect. Furthermore, these transverse strains come with transverse shear and normal stresses that, for equilibrium reasons, are continuous at the each layer interface. These equilibrium conditions are known as Interlaminar Continuity (IC) for transverse stresses. Such discontinuities make difficult the use of classical theories such as Kirchhoff[1] or Reissner–Mindlin[2,3] type theories (to trace accurate responses of sandwich structures, see the books by Zenkert[4] and Vinson[5]).

Several possibilities are known to take ZZ and IC into account in the multilayered structures. Developments,[6,7] have been made in both of Layer-Wise Models[a] (LWM) and Equivalent Single Layer Models[b] framework. The resulting theories are often known as Zig-Zag Theories (ZZT).

Among the ZZTs that have been developed in the ESLM framework, three independent approaches are known. These were denoted in Carrera[8] as, the Lekhnitskii Multilayered Theory (LMT), the

[1]Departamento de Engenharia Mecânica, Faculdade de Engenharia da Universidade do Porto, Rua Dr. Roberto Frias, 4200-465 Porto, Portugal.
[2]INEGI, Faculdade de Engenharia da Universidade do Porto, Rua Dr. Roberto Frias, 4200-465 Porto, Portugal.
[3]Departament of Aeronautics and Aerospace Engineering, Politecnico di Torino, Corso Duca degli Abruzzi, 24, 10129 Torino, Italy.
[4]Université Paris Ouest Nanterre La Défense, Nanterre, 50 rue de Sevres, 92410 Ville d'Avray, France.

Corresponding author:
A.J.M. Ferreira, Departamento de Engenharia Mecânica, Faculdade de Engenharia da Universidade do Porto, Rua Dr. Roberto Frias, 4200-465 Porto, Portugal
Email: ferreira@fe.up.pt

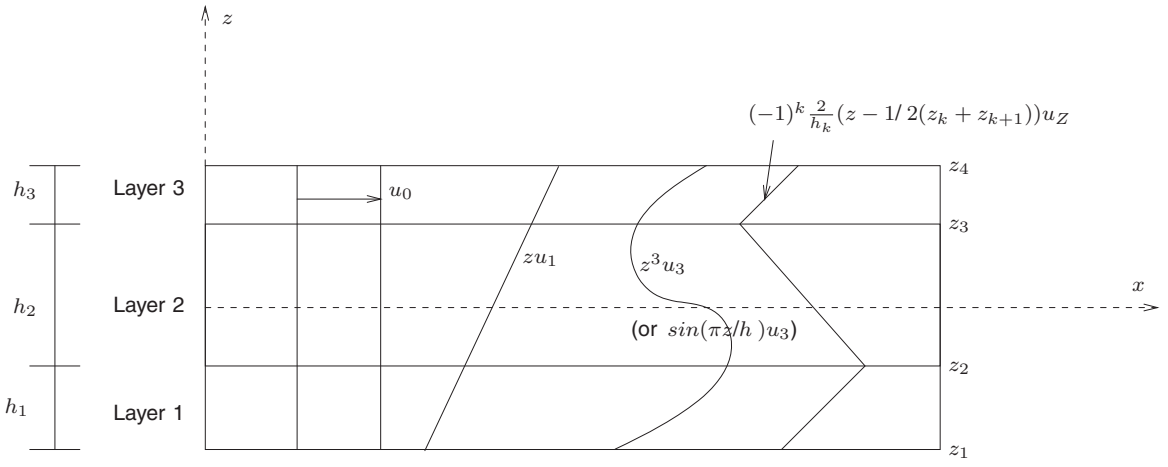

Figure 1. Scheme of the ZZ assumptions for a three-layered laminate.

Ambartsumian Multilayered Theory (AMT), and the Reissner Multilayered Theory (RMT), respectively. The LMT and AWT describe the ZZ effect by enforcing IC via constitutive equations of the layer along with strain–displacement relations. Independent assumptions for displacement and transverse stresses are instead made in the RMT applications.

In the framework of RMT applications, Murakami[9] introduced a function of the thickness coordinate that is able to emulate the ZZ effect. Such a function was denoted in Carrera[10] as the 'Murakami's Zig-Zag Function' (MZZF). The MZZF was used in Murakami[9] and Carrera[10,11] to analyze the static response of layered plates and shells. The Unified Formulation by Carrera (CUF), that have been detailed in Carrera[12] was used to provide a concise framework for developing plate/shell models. Mixed finite elements were developed in Meyer-Piening and Rao[13] and Carrera and Demasi[14] for plates and shells. The MZZF was also applied in the framework of plate/shell theories with only displacement variables,[11,15] see also the review made in Carrera.[10] Other more recent CUF implementations are those in Carrera,[16] applications to sandwich structures have been given.[17–21]

From an implementation point of view, the inclusion of the MZZF in existing plate/shell/beam models requires the same effort as those that are required to include an additional higher-order term (by means of a higher-order polynomial of the thickness coordinate). On the other hand, from a numerical point of view, as will be demonstrated in this article, the MZZF leads to significant improvements of the existing plate/theories; these improvements are difficult to obtained when using other functions that differ from the MZZF.

In this study, the attention is restricted to the application of ZZF to bending, vibration, and buckling analysis of laminated plates by collocation with radial basis functions (RBFs). New displacement theories using two higher order variations of the MZZF and a quadratic variation of the transverse displacements are proposed.

Recently, RBFs have enjoyed considerable success and research as a technique for interpolating data and functions. A RBF, $\phi(|x - x_j|)$ is a spline that depends on the Euclidian distance between distinct data centers x_j, $j = 1, 2, \ldots, N \in \mathbb{R}^n$, also called nodal or collocation points. Although most work to date on RBFs relates to scattered data approximation and in general to interpolation theory, there has recently been an increased interest in their use for solving partial differential equations (PDEs). This approach, which approximates the whole solution of the PDE directly using RBFs, is truly a mesh-free technique. Kansa[22] introduced the concept of solving PDEs by an unsymmetric RBF collocation method based upon the multi quadratic (MQ) interpolation functions, in which the shape parameter may vary across the problem domain. The use of alternative methods to the finite element methods for the analysis of plates, such as the meshless methods based on RBFs is atractive due to the absence of a mesh and the ease of collocation methods. The use of RBF for the analysis of structures and materials has been previously studied by numerous authors.[23–36] A very interesting new technique that may provide excellent results for laminated plates in a near future was recently proposed by Liu and colleagues.[37–42] The authors have recently applied the RBF collocation to the static deformations of composite beams and plates.[43–45]

In a recent authors' work[46] the Unified Formulation has been combined with RBFs to the analysis of thick laminated plates. Attention was restricted to third-and second-order displacement fields for the in-plane and out-of plane components, respectively. The obtained good results has encouraged the research work that is in this article documented. Two higher-order variations

of the MZZF, allowing for through-the-thickness deformations are in this article extended by the use of Unified Formulation and Radial Basis. The first refined model consists of a third-order plus ZZF displacement field for the in-plane components and quadratic transverse for displacement component. The sinus function, that was used by Touratier,[47] Vidal and Polit,[48] replaces the cubic terms in the second refined model. A meshless formulation of higher-order theories is therefore obtained which could be used to provide strong form solutions for plates with various geometries and boundary conditions.

The quality of this method in predicting static deformations, free vibrations, and buckling loads of thin and thick laminated plates is compared and discussed with other methods in some numerical examples.

Two higher order ZZ shear deformation theories

Let us consider a laminated plate composed of perfectly bonded layers, being z the thickness coordinate of the whole plate while z_k is the layer thickness coordinate. a and h are length and thickness of the square laminated plate, respectively. The adimensioned layer coordinate $\zeta_k = (2z_k)/h_k$ is further introduced (h_k is the thickness of the k-th layer). The MZZF $Z(z)$ was defined according to the following formula[9]

$$Z(z) = (-1)^k \zeta_z \tag{1}$$

$Z(z)$ has the following properties:

1. It is a piece-wise linear function of layer coordinates z_k,
2. $Z(z)$ has unit amplitude for the whole layers, and
3. the slope $Z'(z) = \frac{dZ}{dz}$ assumes opposite sign between two adjacent layers. Its amplitude is layer-thickness independent.

A possible FSDT theory has been investigated by Carrera[16] and Demasi,[49] ignoring the through-the-thickness deformations:

$$u = u_0 + zu_1 + (-1)^k \frac{2}{h_k}\left(z - \frac{1}{2}(z_k + z_{k+1})\right)u_Z \tag{2}$$

$$v = v_0 + zv_1 + (-1)^k \frac{2}{h_k}\left(z - \frac{1}{2}(z_k + z_{k+1})\right)v_Z \tag{3}$$

$$w = w_0 \tag{4}$$

The additional degrees of freedom u_Z, v_z have a meaning of displacement, and its amplitude is layer independent.

A refinement of FSDT by inclusion of ZZ effects and transverse normal strains was introduced in Murakami's original ZZF, defined by the following displacement field:

$$u = u_0 + zu_1 + (-1)^k \frac{2}{h_k}\left(z - \frac{1}{2}(z_k + z_{k+1})\right)u_Z \tag{5}$$

$$v = v_0 + zv_1 + (-1)^k \frac{2}{h_k}\left(z - \frac{1}{2}(z_k + z_{k+1})\right)v_Z \tag{6}$$

$$w = w_0 + zw_1 + (-1)^k \frac{2}{h_k}\left(z - \frac{1}{2}(z_k + z_{k+1})\right)w_Z \tag{7}$$

Two higher order variations of the Murakami's ZZ theory are here considered: a theory considering linear, cubic and ZZ terms, and a theory considering linear, sinusoidal and ZZ terms. Both theories consider a quadratic expansion of the transverse displacement in the thickness direction, unlike the Murakami's original theory that considered the same expansion in w as in u, v.

The present HSDT shear deformation theory involves the following expansion of displacements

$$u = u_0 + zu_1 + z^3u_3 + (-1)^k \frac{2}{h_k}\left(z - \frac{1}{2}(z_k + z_{k+1})\right)u_Z \tag{8}$$

$$v = v_0 + zv_1 + z^3v_3 + (-1)^k \frac{2}{h_k}\left(z - \frac{1}{2}(z_k + z_{k+1})\right)v_Z \tag{9}$$

$$w = w_0 + zw_1 + z^2w_2 \tag{10}$$

The present sinus shear deformation theory involves the following expansion of displacements

$$u = u_0 + zu_1 + \sin\left(\frac{\pi z}{h}\right)u_3 + (-1)^k \frac{2}{h_k}\left(z - \frac{1}{2}(z_k + z_{k+1})\right)u_Z \tag{11}$$

$$v = v_0 + zv_1 + \sin\left(\frac{\pi z}{h}\right)v_3 + (-1)^k \frac{2}{h_k}\left(z - \frac{1}{2}(z_k + z_{k+1})\right)v_Z \tag{12}$$

$$w = w_0 + zw_1 + z^2w_2 \tag{13}$$

where u_0, v_0, and w_0 are translations of a point at the middle-surface of the plate, w_2 is higher order translations, and u_1, v_1, u_3, and v_3 denote rotations. This theory is an expansion of early developments by Touratier,[47,50,51] and Vidal and Polit.[48] It considers a quadratic variation of the transverse displacement w, allowing for through-the-thickness deformations.

Review of the unified formulation

In this section, the CUF[10,52–54,] is briefly reviewed. It is shown how to obtain the fundamental nuclei, which allows the derivation of the equations of motion and boundary conditions, in weak form for the finite element analysis; and in strong form for the present RBF collocation.

Governing equations and boundary conditions in the framework of unified formulation

Although one can use the UF for one-layer , isotropic plate, a multi-layered plate with N_l layers is considered. The Principle of Virtual Displacements (PVD) for the pure-mechanical case reads:

$$\sum_{k=1}^{N_l} \int_{\Omega_k} \int_{A_k} \left\{ \delta \epsilon_{pG}^{k\,T} \sigma_{pC}^{k} + \delta \epsilon_{nG}^{k\,T} \sigma_{nC}^{k} \right\} \mathrm{d}\Omega_k \mathrm{d}z = \sum_{k=1}^{N_l} \delta L_e^k \quad (14)$$

where Ω_k and A_k are the integration domains in plane (x,y) and z direction, respectively. Here, k indicates the layer and T the transpose of a vector, and δL_e^k is the external work for the k-th layer. G means geometrical relations and C constitutive equations.

The steps to obtain the governing equations are:

- substitution of the geometrical relations (subscript G);
- substitution of the appropriate constitutive equations (subscript C); and
- introduction of the Unified Formulation.

Stresses and strains are separated into in-plane and normal components, denoted respectively by the subscripts p and n. The mechanical strains in the k-th layer can be related to the displacement field $\mathbf{u}^k = \{u_x^k, u_y^k, u_z^k\}$ via the geometrical relations:

$$\begin{aligned} \epsilon_{pG}^k &= [\epsilon_{xx}, \epsilon_{yy}, \gamma_{xy}]^{kT} = \mathbf{D}_p^k \mathbf{u}^k \,, \\ \epsilon_{nG}^k &= [\gamma_{xz}, \gamma_{yz}, \epsilon_{zz}]^{kT} = (\mathbf{D}_{np}^k + \mathbf{D}_{nz}^k)\, \mathbf{u}^k \,, \end{aligned} \quad (15)$$

wherein the differential operator arrays are defined as follows:

$$\mathbf{D}_p^k = \begin{bmatrix} \partial_x & 0 & 0 \\ 0 & \partial_y & 0 \\ \partial_y & \partial_x & 0 \end{bmatrix}, \quad \mathbf{D}_{np}^k = \begin{bmatrix} 0 & 0 & \partial_x \\ 0 & 0 & \partial_y \\ 0 & 0 & 0 \end{bmatrix}, \quad \mathbf{D}_{nz}^k = \begin{bmatrix} \partial_z & 0 & 0 \\ 0 & \partial_z & 0 \\ 0 & 0 & \partial_z \end{bmatrix}, \quad (16)$$

The 3D constitutive equations are given as:

$$\sigma_{pC}^k = \mathbf{C}_{pp}^k \epsilon_{pG}^k + \mathbf{C}_{pn}^k \epsilon_{nG}^k \sigma_{nG}^k \quad \sigma_{nC}^k = \mathbf{C}_{np}^k \epsilon_{pG}^k + \mathbf{C}_{nn}^k \epsilon_{nG}^k \quad (17)$$

with

$$\mathbf{C}_{pp}^k = \begin{bmatrix} C_{11} & C_{12} & C_{16} \\ C_{12} & C_{22} & C_{26} \\ C_{16} & C_{26} & C_{66} \end{bmatrix} \quad \mathbf{C}_{pn}^k = \begin{bmatrix} 0 & 0 & C_{13} \\ 0 & 0 & C_{23} \\ 0 & 0 & C_{36} \end{bmatrix}$$
$$\mathbf{C}_{np}^k = \begin{bmatrix} 0 & 0 & 0 \\ 0 & 0 & 0 \\ C_{13} & C_{23} & C_{36} \end{bmatrix} \quad \mathbf{C}_{nn}^k = \begin{bmatrix} C_{55} & C_{45} & 0 \\ C_{45} & C_{44} & 0 \\ 0 & 0 & C_{33} \end{bmatrix} \quad (18)$$

According to the CUF, the three displacement components u_x, u_y, and u_z and their relative variations can be modeled as:

$$\begin{aligned} (u_x, u_y, u_z) &= F_\tau \, (u_{x\tau}, u_{y\tau}, u_{z\tau}) \\ (\delta u_x, \delta u_y, \delta u_z) &= F_s \, (\delta u_{xs}, \delta u_{ys}, \delta u_{zs}) \end{aligned} \quad (19)$$

with Taylor expansions from first up to fourth order: $F_0 = z^0 = 1$, $F_1 = z^1 = z, \ldots$, $F_N = z^N, \ldots$, $F_4 = z^4$ if an equivalent single layer (ESL) approach is used.

In Figure 2, it is shown the assembling procedures on layer k for ESL approach.

Substituting the geometrical relations, the constitutive equations and the unified formulation into the variational statement PVD, for the k-th layer, one has:

$$\begin{aligned} \int_{\Omega_k} \int_{A_k} \Big[& (\mathbf{D}_p^k F_s \delta \mathbf{u}_s^k)^T (\mathbf{C}_{pp}^k \mathbf{D}_p^k F_\tau \mathbf{u}_\tau^k + \mathbf{C}_{pn}^k (\mathbf{D}_{n\Omega}^k + \mathbf{D}_{nz}^k) F_\tau \mathbf{u}_\tau^k) \\ & + ((\mathbf{D}_{n\Omega}^k + \mathbf{D}_{nz}^k) F_s \delta \mathbf{u}_s^k)^T (\mathbf{C}_{np}^k \mathbf{D}_p^k F_\tau \mathbf{u}_\tau^k \\ & + \mathbf{C}_{nn}^k (\mathbf{D}_{n\Omega}^k + \mathbf{D}_{nz}^k) F_\tau \mathbf{u}_\tau^k) \Big] \mathrm{d}\Omega_k \mathrm{d}z = \delta L_e^k \end{aligned} \quad (20)$$

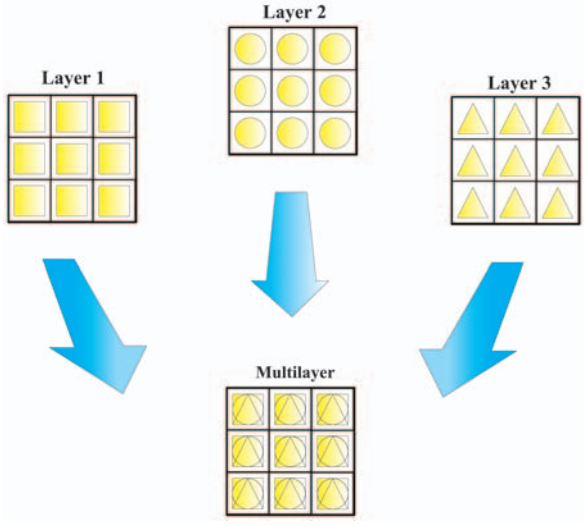

Figure 2. Assembling procedure for ESL approach.

At this point, the formula of integration by parts is applied:

$$\int_{\Omega_k}\left((\mathbf{D}_\Omega)\delta\mathbf{a}^k\right)^T\mathbf{a}^k\mathrm{d}\Omega_k=-\int_{\Omega_k}\delta\mathbf{a}^{kT}\left((\mathbf{D}_\Omega^T)\mathbf{a}^k\right)\mathrm{d}\Omega_k+\int_{\Gamma_k}\delta\mathbf{a}^{kT}\left((\mathbf{I}_\Omega)\mathbf{a}^k\right)\mathrm{d}\Gamma_k \tag{21}$$

where $\mathbf{I}_\Omega$ matrix is obtained applying the *Gradient theorem*:

$$\int_\Omega\frac{\partial\psi}{\partial x_i}\mathrm{d}\upsilon=\oint_\Gamma n_i\psi\mathrm{d}s \tag{22}$$

being n_i the components of the normal $\widehat{n}$ to the boundary along the direction i. After integration by parts, the governing equations and boundary conditions for the plate in the mechanical case are obtained:

$$\begin{aligned}&\int_{\Omega_k}\int_{A_k}(\,\delta\mathbf{u}_s^k)^T\Big[\Big(\big(-\mathbf{D}_p^k\big)^T\big(\mathbf{C}_{pp}^k(\mathbf{D}_p^k)\;+\mathbf{C}_{pn}^k(\mathbf{D}_{n\Omega}^k+\mathbf{D}_{nz}^k)\\&+\big(-\mathbf{D}_{n\Omega}^k+\mathbf{D}_{nz}^k\big)^T\big(\mathbf{C}_{np}^k(\mathbf{D}_p^k)\\&+\mathbf{C}_{nn}^k(\mathbf{D}_{n\Omega}^k+\mathbf{D}_{nz}^k)\big)\Big)\mathbf{F}_\tau\mathbf{F}_s\mathbf{u}_\tau^k\Big]\mathrm{d}x\mathrm{d}y\mathrm{d}z\\&+\int_{\Omega_k}\int_{A_k}(\,\delta\mathbf{u}_s^k)^T\Big[\Big(\mathbf{I}_p^{kT}\big(\mathbf{C}_{pp}^k(\mathbf{D}_p^k)\;+\mathbf{C}_{pn}^k(\mathbf{D}_{n\Omega}^k+\mathbf{D}_{nz}^k)\big)\\&+\mathbf{I}_{np}^{kT}\big(\mathbf{C}_{np}^k(\mathbf{D}_p^k)\;+\mathbf{C}_{nn}^k(\mathbf{D}_{n\Omega}^k+\mathbf{D}_{nz}^k)\big)\Big)\mathbf{F}_\tau\mathbf{F}_s\mathbf{u}_\tau^k\Big]\mathrm{d}x\mathrm{d}y\mathrm{d}z\\&=\int_{\Omega_k}\delta\mathbf{u}_s^{kT}F_s\mathbf{p}_u^k\,\mathrm{d}\Omega_k.\end{aligned} \tag{23}$$

where $\mathbf{I}_p^k$ and $\mathbf{I}_{np}^k$ depend on the boundary geometry:

$$\mathbf{I}_p^k=\begin{bmatrix}n_x&0&0\\0&n_y&0\\n_y&n_x&0\end{bmatrix},\quad\mathbf{I}_{np}^k=\begin{bmatrix}0&0&n_x\\0&0&n_y\\0&0&0\end{bmatrix}. \tag{24}$$

The normal to the boundary of domain Ω is:

$$\widehat{\mathbf{n}}=\begin{bmatrix}n_x\\n_y\end{bmatrix}=\begin{bmatrix}\cos(\varphi_x)\\\cos(\varphi_y)\end{bmatrix} \tag{25}$$

where φ_x and φ_y are the angles between the normal $\widehat{n}$ and the direction x and y, respectively.

The governing equations for a multi-layered plate subjected to mechanical loadings are:

$$\delta\mathbf{u}_s^{kT}:\;\mathbf{K}_{uu}^{k\tau s}\,\mathbf{u}_\tau^k=\mathbf{P}_{u\tau}^k \tag{26}$$

where the fundamental nucleus $\mathbf{K}_{uu}^{k\tau s}$ is obtained as:

$$\begin{aligned}\mathbf{K}_{uu}^{k\tau s}=&\Big[\big(-\mathbf{D}_p^k\big)^T\big(\mathbf{C}_{pp}^k(\mathbf{D}_p^k)+\mathbf{C}_{pn}^k(\mathbf{D}_{n\Omega}^k+\mathbf{D}_{nz}^k)\\&+\big(-\mathbf{D}_{n\Omega}^k+\mathbf{D}_{nz}^k\big)^T\big(\mathbf{C}_{np}^k(\mathbf{D}_p^k)+\mathbf{C}_{nn}^k(\mathbf{D}_{n\Omega}^k+\mathbf{D}_{nz}^k)\big)\Big]\mathbf{F}_\tau\mathbf{F}_s\end{aligned} \tag{27}$$

and the corresponding Neumann-type boundary conditions on Γ_k are:

$$\mathbf{\Pi}_d^{k\tau s}\,\mathbf{u}_\tau^k=\mathbf{\Pi}_d^{k\tau s}\,\bar{\mathbf{u}}_\tau^k\,, \tag{28}$$

where:

$$\begin{aligned}\mathbf{\Pi}_d^{k\tau s}=&\Big[\mathbf{I}_p^{kT}\big(\mathbf{C}_{pp}^k(\mathbf{D}_p^k)\;+\mathbf{C}_{pn}^k(\mathbf{D}_{n\Omega}^k+\mathbf{D}_{nz}^k)\big)+\\&\mathbf{I}_{np}^{kT}\big(\mathbf{C}_{np}^k(\mathbf{D}_p^k)\;+\mathbf{C}_{nn}^k(\mathbf{D}_{n\Omega}^k+\mathbf{D}_{nz}^k)\big)\Big]\mathbf{F}_\tau\mathbf{F}_s\end{aligned} \tag{29}$$

and $\mathbf{P}_{u\tau}^k$ are variationally consistent loads with applied pressure.

Fundamental nuclei

The fundamental nuclei in explicit form are then obtained as:

$$\begin{aligned}K_{uu_{11}}^{k\tau s}&=(-\partial_x^\tau\partial_x^s C_{11}-\partial_x^\tau\partial_y^s C_{16}+\partial_z^\tau\partial_z^s C_{55}\\&\quad-\partial_y^\tau\partial_x^s C_{16}-\partial_y^\tau\partial_y^s C_{66})F_\tau F_s\\K_{uu_{12}}^{k\tau s}&=(-\partial_x^\tau\partial_y^s C_{12}-\partial_x^\tau\partial_x^s C_{16}+\partial_z^\tau\partial_z^s C_{45}\\&\quad-\partial_y^\tau\partial_y^s C_{26}-\partial_y^\tau\partial_x^s C_{66})F_\tau F_s\\K_{uu_{13}}^{k\tau s}&=(-\partial_x^\tau\partial_z^s C_{13}-\partial_y^\tau\partial_z^s C_{36}+\partial_z^\tau\partial_y^s C_{45}+\partial_z^\tau\partial_x^s C_{55})F_\tau F_s\\K_{uu_{21}}^{k\tau s}&=(-\partial_y^\tau\partial_x^s C_{12}-\partial_y^\tau\partial_y^s C_{26}+\partial_z^\tau\partial_z^s C_{45}-\partial_x^\tau\partial_x^s C_{16}\\&\quad-\partial_x^\tau\partial_y^s C_{66})F_\tau F_s\\K_{uu_{22}}^{k\tau s}&=(-\partial_y^\tau\partial_y^s C_{22}-\partial_y^\tau\partial_x^s C_{26}+\partial_z^\tau\partial_z^s C_{44}-\partial_x^\tau\partial_y^s C_{26}\\&\quad-\partial_x^\tau\partial_x^s C_{66})F_\tau F_s\\K_{uu_{23}}^{k\tau s}&=(-\partial_y^\tau\partial_z^s C_{23}-\partial_x^\tau\partial_z^s C_{36}+\partial_z^\tau\partial_y^s C_{44}+\partial_z^\tau\partial_x^s C_{45})F_\tau F_s\\K_{uu_{31}}^{k\tau s}&=(\partial_z^\tau\partial_x^s C_{13}+\partial_z^\tau\partial_y^s C_{36}-\partial_y^\tau\partial_z^s C_{45}-\partial_x^\tau\partial_z^s C_{55})F_\tau F_s\\K_{uu_{32}}^{k\tau s}&=(\partial_z^\tau\partial_y^s C_{23}+\partial_z^\tau\partial_x^s C_{36}-\partial_y^\tau\partial_z^s C_{44}-\partial_x^\tau\partial_z^s C_{45})F_\tau F_s\\K_{uu_{33}}^{k\tau s}&=(\partial_z^\tau\partial_z^s C_{33}-\partial_y^\tau\partial_y^s C_{44}-\partial_y^\tau\partial_x^s C_{45}-\partial_x^\tau\partial_y^s C_{45}\\&\quad-\partial_x^\tau\partial_x^s C_{55})F_\tau F_s\end{aligned} \tag{30}$$

$$\begin{aligned}\Pi_{11}^{k\tau s}&=(n_x\partial_x^s C_{11}+n_x\partial_y^s C_{16}+n_y\partial_x^s C_{16}+n_y\partial_y^s C_{66})F_\tau F_s\\\Pi_{12}^{k\tau s}&=(n_x\partial_y^s C_{12}+n_x\partial_x^s C_{16}+n_y\partial_y^s C_{26}+n_y\partial_x^s C_{66})F_\tau F_s\\\Pi_{13}^{k\tau s}&=(n_x\partial_z^s C_{13}+n_y\partial_z^s C_{36})F_\tau F_s\\\Pi_{21}^{k\tau s}&=(n_y\partial_x^s C_{12}+n_y\partial_y^s C_{26}+n_x\partial_x^s C_{16}+n_x\partial_y^s C_{66})F_\tau F_s\\\Pi_{22}^{k\tau s}&=(n_y\partial_y^s C_{22}+n_y\partial_x^s C_{26}+n_x\partial_y^s C_{26}+n_x\partial_x^s C_{66})F_\tau F_s\\\Pi_{23}^{k\tau s}&=(n_y\partial_z^s C_{23}+n_x\partial_z^s C_{36})F_\tau F_s\\\Pi_{31}^{k\tau s}&=(n_y\partial_z^s C_{45}+n_x\partial_z^s C_{55})F_\tau F_s\\\Pi_{32}^{k\tau s}&=(n_y\partial_z^s C_{44}+n_x\partial_z^s C_{45})F_\tau F_s\\\Pi_{33}^{k\tau s}&=(n_y\partial_y^s C_{44}+n_y\partial_x^s C_{45}+n_x\partial_y^s C_{45}+n_x\partial_x^s C_{55})F_\tau F_s\end{aligned} \tag{31}$$

Dynamic governing equations

The PVD for the dynamic case is expressed as:

$$\sum_{k=1}^{N_l} \int_{\Omega_k} \int_{A_k} \left\{ \delta \epsilon_{pG}^{k\ T} \sigma_{pC}^{k} + \delta \epsilon_{nG}^{k\ T} \sigma_{nC}^{k} \right\} \mathrm{d}\Omega_k \mathrm{d}z = \sum_{k=1}^{N_l} \int_{\Omega_k} \int_{A_k} \rho^k \delta \mathbf{u}^{kT} \ddot{\mathbf{u}}^k \mathrm{d}\Omega_k \mathrm{d}z + \sum_{k=1}^{N_l} \delta L_e^k \tag{32}$$

where ρ^k is the mass density of the k-th layer and double dots denote acceleration.

By substituting the geometrical relations, the constitutive equations and the Unified Formulation, we obtain the following governing equations:

$$\delta \mathbf{u}_s^{k\ T} : \mathbf{K}_{uu}^{k\tau s} \mathbf{u}_\tau^k = \mathbf{M}^{k\tau s} \ddot{\mathbf{u}}_\tau^k + \mathbf{P}_{u\tau}^k \tag{33}$$

In the case of free vibrations one has:

$$\delta \mathbf{u}_s^{k\ T} : \mathbf{K}_{uu}^{k\tau s} \mathbf{u}_\tau^k = \mathbf{M}^{k\tau s} \ddot{\mathbf{u}}_\tau^k \tag{34}$$

where $\mathbf{M}^{k\tau s}$ is the fundamental nucleus for the inertial term. The explicit form of that is:

$$\begin{aligned} M_{11}^{k\tau s} &= \rho^k F_\tau F_s \\ M_{12}^{k\tau s} &= 0 \\ M_{13}^{k\tau s} &= 0 \\ M_{21}^{k\tau s} &= 0 \\ M_{22}^{k\tau s} &= \rho^k F_\tau F_s \\ M_{23}^{k\tau s} &= 0 \\ M_{31}^{k\tau s} &= 0 \\ M_{32}^{k\tau s} &= 0 \\ M_{33}^{k\tau s} &= \rho^k F_\tau F_s \end{aligned} \tag{35}$$

The geometrical and mechanical boundary conditions are the same of the static case.

The RBF method

The static problem

RBFs approximations are mesh-free numerical schemes that can exploit accurate representations of the boundary, are easy to implement and can be spectrally accurate. In this section, the formulation of a global unsymmetrical collocation RBF-based method to compute elliptic operators is presented.

Consider a linear elliptic partial differential operator L and a bounded region Ω in $\mathbb{R}^n$ with some boundary $\partial\Omega$. In the static problems we seek the computation of displacements ($\mathbf{u}$) from the global system of equations

$$\mathcal{L}\mathbf{u} = \mathbf{f} \text{ in } \Omega \tag{36}$$

$$\mathcal{L}_B\mathbf{u} = \mathbf{g} \text{ on } \partial\Omega \tag{37}$$

where $\mathcal{L}$, $\mathcal{L}_B$ are linear operators in the domain and on the boundary, respectively. The right-hand side of Equations (36) and (37) represent the external forces applied on the plate and the boundary conditions applied along the perimeter of the plate, respectively. The PDE problem defined in (36) and (37) will be replaced by a finite problem, defined by an algebraic system of equations, after the radial basis expansions.

The eigenproblem

The eigenproblem looks for eigenvalues (λ) and eigenvectors ($\mathbf{u}$) that satisfy

$$\mathcal{L}\mathbf{u} + \lambda\mathbf{u} = 0 \text{ in } \Omega \tag{38}$$

$$\mathcal{L}_B\mathbf{u} = 0 \text{ on } \partial\Omega \tag{39}$$

As in the static problem, the eigenproblem defined in (38) and (39) is replaced by a finite-dimensional eigenvalue problem, based on RBF approximations.

RBFs approximations

The RBF (ϕ) approximation of a function ($\mathbf{u}$) is given by

$$\widetilde{\mathbf{u}}(\mathbf{x}) = \sum_{i=1}^{N} \alpha_i \phi(\|x - y_i\|_2), \mathbf{x} \in \mathbb{R}^n \tag{40}$$

where y_i, $i = 1,.., N$ is a finite set of distinct points (centers) in $\mathbb{R}^n$. The most common RBFs are

$$\begin{aligned} \text{cubic:} \quad & \phi(r) = r^3 \\ \text{thin plate splines:} \quad & \phi(r) = r^2 \log(r) \\ \text{Wendland functions:} \quad & \phi(r) = (1-r)_+^m p(r) \\ \text{Gaussian:} \quad & \phi(r) = e^{-(cr)^2} \\ \text{multiquadrics:} \quad & \phi(r) = \sqrt{c^2 + r^2} \\ \text{inverse multiquadrics:} \quad & \phi(r) = (c^2 + r^2)^{-1/2} \end{aligned}$$

where the Euclidian distance r is real and non-negative and c is a positive-shape parameter. Hardy[55] introduced multiquadrics in the analysis of scattered geographical data. In the 1990s, Kansa[22] used multiquadrics for the solution of PDEs. Considering

N distinct interpolations, and knowing $u(x_j)$, $j=1, 2,\ldots, N$, we find α_i by the solution of a $N \times N$ linear system

$$\mathbf{A}\boldsymbol{\alpha} = \mathbf{u} \tag{41}$$

where $\mathbf{A} = [\phi(\|x - y_i\|_2)]_{N\times N}$, $\boldsymbol{\alpha} = [\alpha_1, \alpha_2,\ldots, \alpha_N]^T$ and $\mathbf{u} = [u(x_1), u(x_2),\ldots, u(x_N)]^T$.

Solution of the static problem

The solution of a static problem by RBFs considers N_I nodes in the domain and N_B nodes on the boundary, with a total number of nodes $N = N_I + N_B$. We denote the sampling points by $x_i \in \Omega$, $i=1,\ldots, N_I$ and $x_i \in \partial\Omega$, $i = N_I+1,\ldots, N$. At the points in the domain we solve the following system of equations

$$\sum_{i=1}^{N} \alpha_i \mathcal{L}\phi(\|x - y_i\|_2) = \mathbf{f}(x_j), j = 1,2,\ldots,N_I \tag{42}$$

or

$$\mathcal{L}^I\boldsymbol{\alpha} = \mathbf{F} \tag{43}$$

where

$$\mathcal{L}^I = [\mathcal{L}\phi(\|x - y_i\|_2)]_{N_I\times N} \tag{44}$$

At the points on the boundary, we impose boundary conditions as

$$\sum_{i=1}^{N} \alpha_i \mathcal{L}_B\phi(\|x - y_i\|_2) = \mathbf{g}(x_j), j = N_I + 1,\ldots,N \tag{45}$$

or

$$\mathbf{B}\boldsymbol{\alpha} = \mathbf{G} \tag{46}$$

where

$$\mathbf{B} = \mathcal{L}_B\phi\left[\left(\|x_{N_I+1} - y_j\|_2\right)\right]_{N_B\times N}$$

Therefore, we can write a finite-dimensional static problem as

$$\begin{bmatrix} \mathcal{L}^I \\ \mathbf{B} \end{bmatrix}\boldsymbol{\alpha} = \begin{bmatrix} \mathbf{F} \\ \mathbf{G} \end{bmatrix} \tag{47}$$

By inverting the system (47), we obtain the vector $\boldsymbol{\alpha}$. We then obtain the solution $\mathbf{u}$ using the interpolation Equation (40).

Solution of the eigenproblem

We consider N_I nodes in the interior of the domain and N_B nodes on the boundary, with $N = N_I + N_B$. We denote interpolation points by $x_i \in \Omega$, $i=1,\ldots, N_I$ and $x_i \in \partial\Omega$, $i = N_I+1,\ldots, N$. At the points in the domain, we define the eigenproblem as

$$\sum_{i=1}^{N} \alpha_i \mathcal{L}\phi(\|x - y_i\|_2) = \lambda\tilde{\mathbf{u}}(x_j), j = 1,2,\ldots,,N_I \tag{48}$$

or

$$\mathcal{L}^I\boldsymbol{\alpha} = \lambda\tilde{\mathbf{u}}^I \tag{49}$$

where

$$\mathcal{L}^I = [\mathcal{L}\phi(\|x - y_i\|_2)]_{N_I\times N} \tag{50}$$

At the points on the boundary, we enforce the boundary conditions as

$$\sum_{i=1}^{N} \alpha_i \mathcal{L}_B\phi(\|x - y_i\|_2) = 0, j = N_I + 1,\ldots,,N \tag{51}$$

or

$$\mathbf{B}\boldsymbol{\alpha} = 0 \tag{52}$$

Equations (49) and (52) can now be solved as a generalized eigenvalue problem

$$\begin{bmatrix} \mathcal{L}^I \\ \mathbf{B} \end{bmatrix}\boldsymbol{\alpha} = \lambda\begin{bmatrix} \mathbf{A}^I \\ \mathbf{0} \end{bmatrix}\boldsymbol{\alpha} \tag{53}$$

where

$$\mathbf{A}^I = \phi\left[\left(\|x_{N_I} - y_j\|_2\right)\right]_{N_I\times N}$$

Discretization of the equations of motion and boundary conditions

The radial basis collocation method follows a simple implementation procedure. Taking Equation (11), we compute

$$\boldsymbol{\alpha} = \begin{bmatrix} L^I \\ \mathbf{B} \end{bmatrix}^{-1}\begin{bmatrix} \mathbf{F} \\ \mathbf{G} \end{bmatrix} \tag{54}$$

This $\boldsymbol{\alpha}$ vector is then used to obtain solution $\tilde{\mathbf{u}}$, by using (6). If derivatives of $\tilde{\mathbf{u}}$ are needed, such derivatives are computed as

$$\frac{\partial\tilde{\mathbf{u}}}{\partial x} = \sum_{j=1}^{N} \alpha_j \frac{\partial\phi_j}{\partial x} \tag{55}$$

$$\frac{\partial^2\tilde{\mathbf{u}}}{\partial x^2} = \sum_{j=1}^{N} \alpha_j \frac{\partial^2\phi_j}{\partial x^2}, \text{etc.} \tag{56}$$

In the present collocation approach, we need to impose essential and natural boundary conditions. Consider, for example, the condition $w=0$, on a simply supported or clamped edge. We enforce the conditions by interpolating as

$$w = 0 \rightarrow \sum_{j=1}^{N} \alpha_j^W \phi_j = 0 \tag{57}$$

Other boundary conditions are interpolated in a similar way.

Free vibrations problems

For free vibration problems, we set the external force to zero, and assume harmonic solution in terms of displacements u_0, u_1, v_0, v_1,.... Considering the example of the cubic theory, we define

$$\begin{aligned} u_0 &= U_0(w,y)e^{i\omega t}; \quad u_1 = U_1(w,y)e^{i\omega t}; \\ u_3 &= U_3(w,y)e^{i\omega t}; \quad u_Z = U_Z(w,y)e^{i\omega t} \end{aligned} \tag{58}$$

$$\begin{aligned} v_0 &= V_0(w,y)e^{i\omega t}; \quad v_1 = V_1(w,y)e^{i\omega t}; \\ v_3 &= V_3(w,y)e^{i\omega t}; \quad v_Z = V_Z(w,y)e^{i\omega t} \end{aligned} \tag{59}$$

$$\begin{aligned} w_0 &= W_0(w,y)e^{i\omega t}; \quad w_1 = W_1(w,y)e^{i\omega t}; \\ w_2 &= W_2(w,y)e^{i\omega t} \end{aligned} \tag{60}$$

where ω is the frequency of natural vibration. Substituting the harmonic expansion into equations (53) in terms of the amplitudes U_0, U_1, U_3, U_Z, V_0, V_1, V_3, V_Z, W_0, W_1, W_2, we may obtain the natural frequencies and vibration modes for the plate problem, by solving the eigenproblem

$$[\mathcal{L} - \omega^2 \mathcal{G}]\mathbf{X} = \mathbf{0} \tag{61}$$

where $\mathcal{L}$ collects all stiffness terms and $\mathcal{G}$ collects all terms related to the inertial terms. In (61), $\mathbf{X}$ are the modes of vibration associated with the natural frequencies defined as ω.

Buckling analysis

The buckling analysis considers the addition into the equations of motion of terms $\bar{N_{xx}}\frac{\partial^2 w}{\partial x^2} + 2\bar{N_{xy}}\frac{\partial^2 w}{\partial x \partial y} + \bar{N_{yy}}\frac{\partial^2 w}{\partial y^2}$, associated with equation in w_0, being $\bar{N_{xx}}$,$\bar{N_{xy}}$, and $\bar{N_{yy}}$ the in-plane applied forces. In order to determine the critical buckling load of the laminated plate, the transverse load and all inertial terms areset to zero.

The eigenproblem associated with the buckling problem is then defined as

$$[\mathcal{L} - \lambda \mathcal{G}]\mathbf{X} = \mathbf{0} \tag{62}$$

where $\mathcal{L}$ collects all stiffness terms and $\mathcal{G}$ collects all terms related to the in-plane forces. In (62), $\mathbf{X}$ are the buckling modes associated with the buckling loads defined as λ.

Numerical examples

All numerical examples consider a Chebyshev grid and a Wendland function, defined as

$$\phi(r) = (1 - c\ r)_+^8 \left(32(c\ r)^3 + 25(c\ r)^2 + 8c\ r + 1\right) \tag{63}$$

where the shape parameter (c) was obtained by an optimization procedure, as in Ferreira and Fasshauer.[56]

Static problems cross-ply laminated plates

A simply supported square laminated plate of side a and thickness h is composed of four equally layers oriented at [0°/90°/90°/0°]. The plate is subjected to a sinusoidal vertical pressure of the form

$$p_z = P \sin\left(\frac{\pi x}{a}\right) \sin\left(\frac{\pi y}{a}\right)$$

with the origin of the coordinate system located at the lower left corner on the midplane and P the maximum load (at center of plate).

The orthotropic material properties for each layer are given by

$$\begin{aligned} E_1 &= 25.0E_2 \quad G_{12} = G_{13} = 0.5E_2 \\ G_{23} &= 0.2E_2 \quad \nu_{12} = 0.25 \end{aligned}$$

The in-plane displacements, the transverse displacements, the normal stresses and the in-plane and transverse shear stresses are presented in normalized form as

$$\overline{w} = \frac{10^2 w_{(a/2,a/2,0)} h^3 E_2}{Pa^4} \quad \overline{\sigma}_{xx} = \frac{\sigma_{xx(a/2,a/2,h/2)} h^2}{Pa^2}$$

$$\overline{\sigma}_{yy} = \frac{\sigma_{yy(a/2,a/2,h/4)} h^2}{Pa^2}$$

$$\overline{\tau}_{xz} = \frac{\tau_{xz(0,a/2,0)} h}{Pa} \quad \overline{\tau}_{xy} = \frac{\tau_{xy(0,0,h/2)} h^2}{Pa^2}$$

In Table 1, we present results for the present z^3-ZZ and SINUS-ZZ theory, using 11×11 up to 21×21 points. We compare results with higher order solutions by Ahkras et al.[57] and Reddy,[58] FSDT solutions by Reddy and Chao,[59] and an exact solution by Pagano.[60] We also compare with results by the authors using RBFs with Reddy's theory,[45] and a layerwise theory.[61] Both higher order theories produce excellent results, when compared with other HSDT theories, for all a/h ratios, for transverse displacements, normal stresses, and transverse shear stresses. It is clear that the FSDT cannot be used for thick laminates. In Figure 3, the σ_{xx} evolution across the thickness direction is illustrated, for $a/h = 4$, using 21×21 points. The influence of the SINUS-ZZ formulation in the skins is visible. In Figure 4, the τ_{xz} evolution across the thickness direction is illustrated, for $a/h = 4$, using 21×21 points. Note that the transverse shear stresses are obtained directly from the constitutive equations. The parabolic evolution of the stress at the core and skins is quite clear, as expected from the formulation.

Table 1. [0°/90°/90°/0°] square laminated plate under two higher order ZZ formulations

$\frac{a}{h}$	Method	$\overline{w}$	$\overline{\sigma}_{xx}$	$\overline{\sigma}_{yy}$	$\overline{\tau}_{zx}$	$\overline{\tau}_{xy}$
4	HSDT[58]	1.8937	0.6651	0.6322	0.2064	0.0440
	FSDT[59]	1.7100	0.4059	0.5765	0.1398	0.0308
	Elasticity[60]	1.954	0.720	0.666	0.270	0.0467
	SINUS-ZZ					
	Present (13 × 13 grid)	1.9253	0.6920	0.5810	0.2080	0.0418
	Present (17 × 17 grid)	1.9253	0.6920	0.5809	0.2159	0.0418
	Present (21 × 21 grid)	1.9253	0.6920	0.5809	0.2196	0.0418
	z^3-ZZ					
	Present (13 × 13 grid)	1.9231	0.6965	0.6408	0.2058	0.0409
	Present (17 × 17 grid)	1.9231	0.6965	0.6408	0.2136	0.0409
	Present (21 × 21 grid)	1.9231	0.6965	0.6408	0.2173	0.0409
10	HSDT[58]	0.7147	0.5456	0.3888	0.2640	0.0268
	FSDT[59]	0.6628	0.4989	0.3615	0.1667	0.0241
	Elasticity[60]	0.743	0.559	0.403	0.301	0.0276
	SINUS-ZZ					
	Present (13 × 13 grid)	0.7374	0.5626	0.3971	0.2882	0.0263
	Present (17 × 17 grid)	0.7374	0.5627	0.3971	0.2992	0.0263
	Present (21 × 21 grid)	0.7374	0.5627	0.3971	0.3044	0.0263
	z^3-ZZ					
	Present (13 × 13 grid)	0.7225	0.5637	0.3935	0.2616	0.0274
	Present (17 × 17 grid)	0.7225	0.5637	0.3935	0.2715	0.0274
	Present (21 × 21 grid)	0.7225	0.5637	0.3935	0.2762	0.0274
100	HSDT[58]	0.4343	0.5387	0.2708	0.2897	0.0213
	FSDT[59]	0.4337	0.5382	0.2705	0.1780	0.0213
	Elasticity[60]	0.4347	0.539	0.271	0.339	0.0214
	SINUS-ZZ					
	Present (13 × 13 grid)	0.4356	0.5440	0.2743	0.3240	0.0214
	Present (17 × 17 grid)	0.4357	0.5443	0.2738	0.3369	0.0214
	Present (21 × 21 grid)	0.4358	0.5444	0.2737	0.3429	0.0214
	z^3-ZZ					
	Present (13 × 13 grid)	0.4370	0.5434	0.2739	0.2901	0.0215
	Present (17 × 17 grid)	0.4372	0.5438	0.2734	0.3016	0.0215
	Present (21 × 21 grid)	0.4372	0.5438	0.2733	0.3069	0.0215

The SINUS-ZZ theory is better than the z^3-ZZ theory for thicker plates.

Free vibration problems cross-ply laminated plates

In this example, all layers of the laminate are assumed to be of the same thickness, density and made of the same linearly elastic composite material.

The following material parameters of a layer are used:

$$\frac{E_1}{E_2} = 10, 20, 30 \text{ or } 40; \; G_{12} = G_{13} = 0.6E_2;$$
$$G_3 = 0.5E_2; \; \nu_{12} = 0.25$$

The subscripts 1 and 2 denote the directions normal and transverse to the fiber direction in a lamina, which may be oriented at an angle to the plate axes. The ply angle of each layer is measured from the global x-axis to the fiber direction.

The example considered is a simply supported square plate of the cross-ply lamination [0°/90°/90°/0°]. The thickness and length of the plate are denoted by h and a, respectively. The thickness-to-span ratio $h/a = 0.2$ is employed in the computation. Table 2 lists the fundamental frequency of the simply supported laminate made of various modulus ratios of E_1/E_2. Figure 5 illustrates the modes of vibration for $E_1/E_2 = 10$, grid 21 × 21 points. It is found that the present meshless results are in very close agreement with

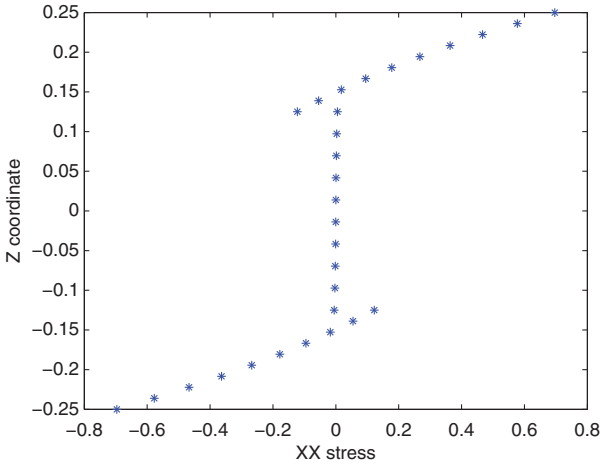

Figure 3. Normalized normal σ_{xx} stress for $a/h = 4$, 21×21 points, z^3-ZZ.

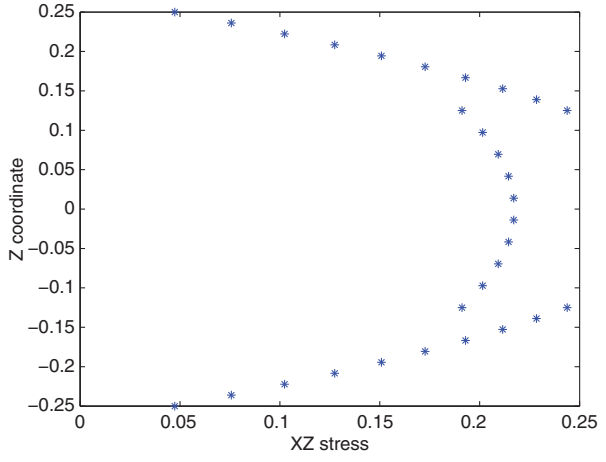

Figure 4. Normalized transverse τ_{xz} stress for $a/h = 4$, 21×21 points, z^3-ZZ.

the values in Refs.[62,63] and the meshfree results of Liew et al.[64] based on the FSDT.

Buckling examples

Three-layer [0°/90°/0°] and four-layer [0°/90°/90°0°] square cross-ply laminates are chosen to compute the uni- and bi-axial buckling loads. The plate has width a and thickness h. The span-to-thickness ratio a/h is taken to be 10. All layers are assumed to be of the same thickness and material properties:

$$E_1/E_2 = 40;\ G_{12}/E_2 = G_{13}/E_2 = 0.6;\ G_{23}/E_2 = 0.5;$$
$$\nu_{12} = 0.25$$

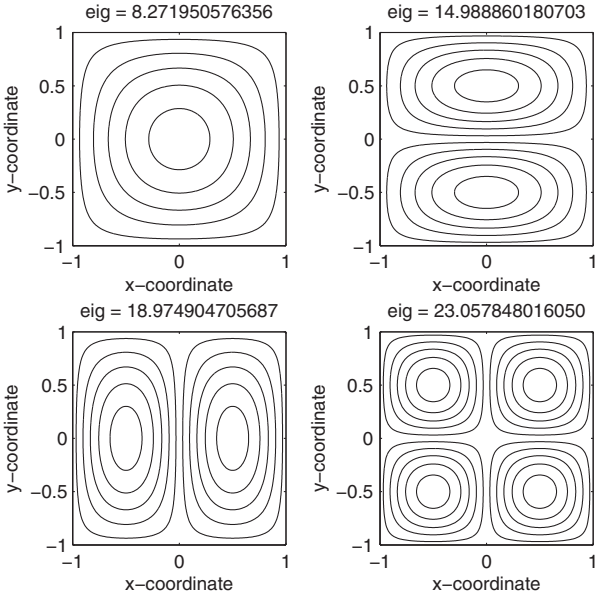

Figure 5. First four modes of vibration of four-layer [0°/90°/90°/0°] simply supported laminated plate ($\bar{w} = (wa^2/h)\sqrt{\rho/E_2}$, $h/a = 0.2$), $E_1/E_2$010, grid 21×21 points, SINUS-ZZ.

Table 2. The normalized fundamental frequency of the simply-supported cross-ply laminated square plate [0°/90°/90°/0°] ($\bar{w} = (wa^2/h)\sqrt{\rho/E_2}$,$h/a = 0.2$)

		E_1/E_2			
Method	Grid	10	20	30	40
Liew[64]		8.2924	9.5613	10.320	10.849
Exact (Reddy[62], Khdeir[63])		8.2982	9.5671	10.326	10.854
Present SINUS-ZZ ($\nu_{23} = 0.25$)	13×13	8.2721	9.5188	10.2483	10.7441
	17×17	8.2720	9.5187	10.2482	10.7440
	21×21	8.2720	9.5187	10.2482	10.7440
Present z^3-ZZ ($\nu_{23} = 0.25$)	13×13	8.2884	9.5359	10.2642	10.7588
	17×17	8.2883	9.5357	10.2641	10.7586
	21×21	8.2883	9.5357	10.2641	10.7586

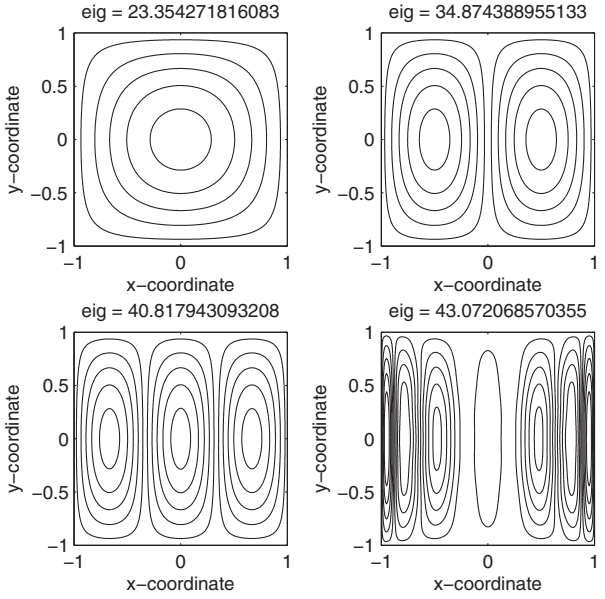

Figure 6. First four buckling modes: Uni-axial buckling load of four-layer [0°/90°/90°/0°] simply supported laminated plate ($\bar{N} = \bar{N}_{xx}a^2/(E_2h^3), \bar{N}_{xy} = 0, \bar{N}_{yy} = 0$), grid 13×13 points, z^3-ZZ.

Table 3. Uni-axial buckling load of four-layer [0°/90°/90°/0°] simply supported laminated plate ($\bar{N} = \bar{N}_{xx}a^2/(E_2h^3)$, $\bar{N}_{xy} = 0, \bar{N}_{yy} = 0$)

Grid	Present	Liew and Huang[66]	Khdeir and Librescu[65]
SINUS-ZZ			
13×13	23.3641	23.463	23.453
17×17	23.3632		
21×21	23.3631		
z^3-ZZ			
13×13	23.3543	23.463	23.453
17×17	23.3534		
21×21	23.3533		

In Figure 6 it is illustrated the first four buckling modes for uni-axial buckling load of four-layer [0°/90°/90°/0°] simply supported laminated plate ($\bar{N} = \bar{N}_{xx}a^2/(E_2h^3), \bar{N}_{xy} = \bar{N}_{yy} = 0$), using a grid of 13×13 points, for the z^3-ZZ formulation.

Table 3 lists the uni-axial buckling loads of the four-layer simply supported laminated plate. Exact solutions by Khdeir and Librescu[65] and differential quadrature results by Liew and Huang[66] based on the FSDT are also presented for comparison. It is found that the critical buckling load is obtained with a few grid points. The present results are in excellent correlation with those of Khdeir and Librescu,[65] and those of Liew and Huang.[66]

Table 4 tabulates the bi-axial buckling loads of the [0°/90°/0°] laminated plate. The laminated plate is simply supported along the edges parallel to the x-axis while the other two edges may be simply supported (S), or clamped (C). The notations SS, SC, and CC refer to the boundary conditions of the two edges parallel to the x-axis only.

Table 4. Bi-axial buckling load of three-layer [0°/90°/0°] simply supported laminated plate ($\bar{N} = \bar{N}_{xx}a^2/(E_2h^3), \bar{N}_{xy} = 0, \bar{N}_{yy} = \bar{N}_{xx}$)

Grid	SS	CC
SINUS-ZZ		
13×13	10.0422	13.2559
17×17	10.0411	13.2549
21×21	10.0410	13.2548
z^3-ZZ		
13×13	10.0430	13.2493
17×17	10.0418	13.2483
21×21	10.0417	13.2482
Liew and Huang[66]	10.178	13.260
Khdeir and Librescu[65]	10.202	13.290

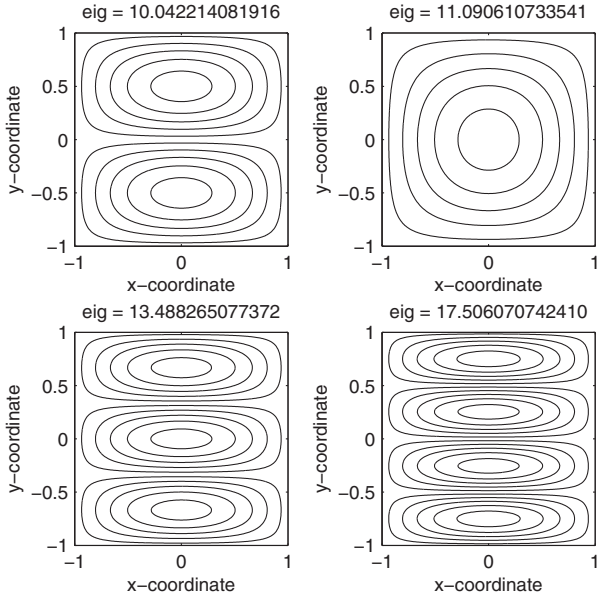

Figure 7. First four buckling modes: Bi-axial buckling load of three-layer [0°/90°/0°] simply supported (SSSS) laminated plate ($\bar{N} = \bar{N}_{xx}a^2/(E_2h^3), \bar{N}_{xy} = 0, \bar{N}_{yy} = \bar{N}_{xx}$), grid 13×13 points, SINUS-ZZ.

In Figure 7, it is illustrated the first four buckling modes for bi-axial buckling load of three-layer [0°/90°/0°] simply supported laminated plate ($\bar{N} = \bar{N}_{xx}a^2/(E_2h^3), \bar{N}_{xy} = 0, \bar{N}_{yy} = \bar{N}_{xx}$), using a grid of 17×17 points, for the SINUS-ZZ formulation.

In Figure 8, it is illustrated the first four buckling modes for bi-axial buckling load of three-layer [0°/90°/0°] SCSC laminated plate ($\bar{N} = \bar{N}_{xx}a^2/(E_2h^3)$,

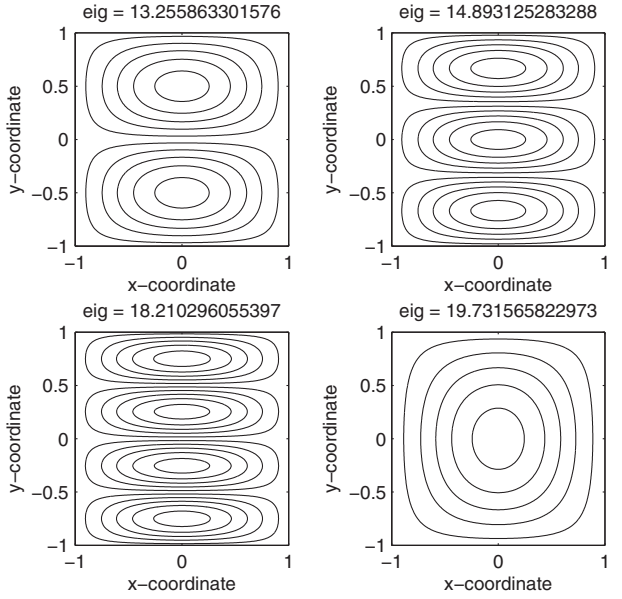

Figure 8. First four buckling modes: Bi-axial buckling load of three-layer [0°/90°/0°] SCSC laminated plate ($\bar{N} = \bar{N}_{xx}a^2/(E_2h^3)$, $\bar{N}_{xy} = 0, \bar{N}_{yy} = \bar{N}_{xx}$), grid 13 × 13 points, SINUS-ZZ.

$\bar{N}_{xy} = 0, \bar{N}_{yy} = \bar{N}_{xx}$, using a grid of 17×17 points, for the SINUS-ZZ formulation.

It is found that excellent agreement is achieved for all edge conditions considered when comparing the results obtained by the present RBF approach with the FSDT solutions by Khadeir and Librescu[65] and those of Liew and Huang,[66] who use a MLSDQ approach. Note that although comparison with other sources are excellent, the critical loads are related to the second mode (SSSS), fourth mode (SCSC), and third mode (SSSC).

Conclusions

In this article, we presented a study using the RBF collocation method to analyze static deformations, free vibrations and buckling loads of thick isotropic and laminated plates using two higher order ZZT, one considering a combination of cubic and ZZ terms, and another considering sinus and ZZ terms. Both theories allow for through-the-thickness deformations. This has not been done before and serves to fill the gap of knowledge in this area of research.

Using the Unified Formulation with the radial basis collocation, all the C^o plate formulations can be easily discretized by RBFs collocation. Also, the burden of deriving the equations of motion and boundary conditions is eliminated with the present approach. All is needed is to change one vector F_t that defines the expansion of displacements.

We analyzed square isotropic and cross-ply laminated plates in bending, free vibrations, and buckling loads. These results were compared with existing analytical solutions or competitive finite element solutions and excellent agreement was observed in all cases.

This meshless formulation shows a similar computational effort with respect to finite elements for static problems, although the eigenproblem takes longer to compute given the unsymmetric nature of the matrices involved.

This present method is a simple yet powerful alternative to other finite element or meshless methods in the static deformation and free vibration analysis of thin and thick isotropic or laminated plates.

Notes

a. The number of the unknown variables is kept dependent on the number of the constitutive layers.
b. The unknown variables are the same for the whole laminate.

References

1. Kirchhoff G. Uber das gleichgewicht und die bewegung einer elastischen scheibe. *J Angew Math* 1850; 40: 51–88.
2. Reissner E. The effect of transverse shear deformations on the bending of elastic plates. *J Appl Mech* 1945; 12: A69–A77.
3. Mindlin RD. Influence of rotary inertia and shear in flexural motions of isotropic elastic plates. *J Appl Mech* 1951; 18: 31–38.
4. Zenkert D. *An introduction to sandwich structures*. Oxford: Chamelon Press, 1995.
5. Vinson JR. *The behavior of sandwich structures of isotropic and composite materials*. Lancaster PA: Technomic Publishing Co, 1999.
6. Lekhnitskii SG. Strength calculation of composite beams. *Vestnik Inzhen i Tekhnikov* 1935; 9.
7. Carrera E. Theories and finite elements for multilayered anisotropic, composite plates and shells. *Arch Comput Methods Eng* 2002; 9: 87–140.
8. Carrera E. Historical review of zig-zag theories for multilayered plates and shells. *Appl Mech Rev* 2003; (56): 287–308.
9. Murakami H. Laminated composite plate theory with improved in-plane responses. *J Appl Mech* 1986; 53: 661–666.
10. Carrera E. Developments, ideas, and evaluations based upon reissner's mixed variational theorem in the modelling of multilayered plates and shells. *Appl Mech Rev* 2001; 54: 301–329.
11. Carrera E. A study of transverse normal stress effects on vibration of multilayered plates and shells. *J Sound Vib* 1999; 225: 803–829.
12. Carrera E. Theories and finite elements for multilayered plates and shells: A unified compact formulation with numerical assessment and benchmarking. *Arch Comput Meth Eng* 2003; 10: 215–297.

13. Meyer-Piening HR and Rao KM. Analysis of thick laminated anisotropic composites plates by the finite element method. *Comp Struct* 1990; 15: 185–213.
14. Carrera E and Demasi L. Multilayered finite plate element based on reissner mixed variational theorem. part i: Theory. and part ii: Numerical analysis. *Int J Numer Methods Eng* 2002; 55: 191–231; 253–291.
15. Varadan TK and Bhaskar K. A higher-order theory for bending analysis of laminated shells of revolution. *Compos Struct* 1991; 40: 815–819.
16. Carrera E. The use of murakamiÕs zig-zag function in the modeling of layered plates and shells. *Compos Struct* 2004; 82: 541–554.
17. Carrera E and Brischetto S. A comparison of various kinematic models for sandwich shell panels with soft core. *J Compos Mater* 2009; 43: 2201–2221.
18. Carrera E and Brischetto S. A survey with numerical assessment of classical and refined theories for the analysis of sandwich plate. *Appl Mech Rev* 2009; 62(1): 1–17.
19. Carrera E, Brischetto S and Demasi L. Improved bending analysis of sandwich plate by using zig-zag function. *Compos Struct* 2009; 89: 408–415.
20. Carrera E, Brischetto S and Demasi L. Improved response of unsymmetrically laminated sandwich plates by using zig-zag functions. *J Sand Struct Mater* 2009; 11(2–3): 257–267.
21. Carrera E, Brischetto S and Demasi L. Free vibration of sandwich plates and shells by using zig-zag function. *Shock Vib* 2009; 16: 495–503.
22. Kansa EJ. Multiquadrics- a scattered data approximation scheme with applications to computational fluid dynamics. i: Surface approximations and partial derivative estimates. *Comput Math Appl* 1990; 19(8/9): 127–145.
23. Hon YC, Lu MW, Xue WM and Zhu YM. Multiquadric method for the numerical solution of byphasic mixture model. *Appl Math Comput* 1997; 88: 153–175.
24. Hon YC, Cheung KF, Mao XZ and Kansa EJ. A multiquadric solution for the shallow water equation. *ASCE J Hydraul Eng* 1999; 125(5): 524–533.
25. Wang JG, Liu GR and Lin P. Numerical analysis of biot's consolidation process by radial point interpolation method. *Int J Solids Struct* 2002; 39(6): 1557–1573.
26. Liu GR and Gu YT. A local radial point interpolation method (lrpim) for free vibration analyses of 2-d solids. *J Sound Vib* 2001; 246(1): 29–46.
27. Liu GR and Wang JG. A point interpolation meshless method based on radial basis functions. *International j Numer Meth Eng* 2002; 54: 1623–1648.
28. Wang JG and Liu GR. On the optimal shape parameters of radial basis functions used for 2-d meshless methods. *Comput Methods Appl Mech Eng* 2002; 191: 2611–2630.
29. Chen XL, Liu GR and Lim SP. An element free galerkin method for the free vibration analysis of composite laminates of complicated shape. *Compos Struct* 2003; 59: 279–289.
30. Dai KY, Liu GR, Lim SP and Chen XL. An element free galerkin method for static and free vibration analysis of shear-deformable laminated composite plates. *J Sound Vib* 2004; 269: 633–652.
31. Liu GR and Chen XL. Buckling of symmetrically laminated composite plates using the element-free galerkin method. *Int J Struct Stab Dyn* 2002; 2: 281–294.
32. Liew KM, Chen XL and Reddy JN. Mesh-free radial basis function method for buckling analysis of non-uniformity loaded arbitrarily shaped shear deformable plates. *Comput Meth Appl Mech Eng* 2004; 193: 205–225.
33. Huang YQ and Li QS. Bending and buckling analysis of antisymmetric laminates using the moving least square differential quadrature method. *Comput Meth Appl Mech Eng* 2004; 193: 3471–3492.
34. Liu L, Liu GR and Tan VCB. Element free method for static and free vibration analysis of spatial thin shell structures. *Comput Meth Appl Mech Eng* 2002; 191: 5923–5942.
35. Xiang S, Wang KM, Ai YT, Sha YD and Shi H. Analysis of isotropic, sandwich and laminated plates by a meshless method and various shear deformation theories. *Compos Struct* 2009; 91(1): 31–37.
36. Xiang S, Shi H, Wang KM, Ai YT and Sha YD. Thin plate spline radial basis functions for vibration analysis of clamped laminated composite plates. *Eur J Mech A/ Solids* 2010; 29: 844–850.
37. Liu GR and Nguyen-Thoi T. *Smoothed finite element Method*. Boca Raton, FL: CRC Press, 2010.
38. Liu GR, Nguyen-Thoi T and Lam KY. An edge-based smoothed finite element method (es-fem) for static, free and forced vibration analyses in solids. *J Sound Vib* 2009; 320: 1100–1130.
39. Nguyen-Xuan H, Liu GR, Thai-Hoang C and Nguyen-Thoi T. An edge-based smoothed finite element method with stabilized discrete shear gap technique for analysis of reissner-mindlin plates. *Comput Meth Appl Mech Eng* 2009; 199: 471–489.
40. Nguyen-Xuan H, Liu GR, Nguyen-Thoi T and Nguyen-Tran C. An edge-based smoothed finite element method for analysis of two-dimensional piezoelectric structures. *Smart Mater Struct* 2009; 18(6): 065015.
41. Nguyen-Thoi T, Liu GR, Vu-Do HC and Nguyen-Xuan H. An edge-based smoothed finite element method (es-fem) for visco-elastoplastic analyses of 2d solids using triangular mesh. *Comput Mech* 2009; 45: 23–44.
42. Nguyen-Thoi T, Liu GR and Nguyen-Xuan H. An n-sided polygonal edge-based smoothed finite element method (nes-fem) for solid mechanics. *Int J Numer Methods Biomed Eng* 2010; doi:10.1002/cnm.1375.
43. Ferreira AJM. A formulation of the multiquadric radial basis function method for the analysis of laminated composite plates. *Compos Struct* 2003; 59: 385–392.
44. Ferreira AJM. Thick composite beam analysis using a global meshless approximation based on radial basis functions. *Mech Adv Mater Struct* 2003; 10: 271–284.
45. Ferreira AJM, Roque CMC and Martins PALS. Analysis of composite plates using higher-order shear deformation theory and a finite point formulation based on the multiquadric radial basis function method. *Composites: Part B* 2003; 34: 627–636.
46. Ferreira AJM, Roque CMC, Carrera E and Cinefra M. Analysis of thick isotropic and cross-ply laminated plates

by radial basis functions and unified formulation. *J Sound Vib* 2011; 330(4): 771–787.
47. Touratier M. An efficient standard plate theory. *Int J Eng Sci* 1991; 29: 901–916.
48. Vidal P and Polit O. A family of sinus finite elements for the analysis of rectangular laminated beams. *Compos Struct* 2008; 84: 56–72.
49. Demasi L. ∞^3 hierarchy plate theories for thick and thin composite plates: the generalized unified formulation. *Compos Struct* 2008; 84: 256–270.
50. Touratier M. A generalization of shear deformation theories for axisymmetric multilayered shells. *Int J Solids Struct* 1992; 29: 1379–1399.
51. Touratier M. A refined theory of laminated shallow shells. *Int J Solids Struct* 1992; 29(11): 1401–1415.
52. Carrera E. C^0 reissner-mindlin multilayered plate elements including zig-zag and interlaminar stress continuity. *Int J Numer Meth Eng* 1996; 39: 1797–1820.
53. Carrera E and Kroplin B. Zig-zag and interlaminar equilibria effects in large deflection and post-buckling analysis of multilayered plates. *Mech Compos Mater Struct* 1997; 4: 69–94.
54. Carrera E. Evaluation of layer-wise mixed theories for laminated plate analysis. *AIAA J* 1998; 36: 830–839.
55. Hardy RL. Multiquadric equations of topography and other irregular surfaces. *Geophys Res* 1971; 176: 1905–1915.
56. Ferreira AJM and Fasshauer GE. Computation of natural frequencies of shear deformable beams and plates by a rbf-pseudospectral method. *Comput Methods Appl Mech Eng* 2006; 196: 134–146.
57. Akhras G, Cheung MS and Li W. Finite strip analysis for anisotropic laminated composite plates using higher-order deformation theory. *Comput Struct* 1994; 52(3): 471–477.
58. Reddy JN. A simple higher-order theory for laminated composite plates. *J Appl Mech* 1984; 51: 745–752.
59. Reddy JN and Chao WC. A comparison of closed-form and finite-element solutions of thick laminated anisotropic rectangular plates. *Nucl Eng Des* 1981; 64: 153–167.
60. Pagano NJ. Exact solutions for rectangular bidirectional composites and sandwich plates. *J Compos Mater* 1970; 4: 20–34.
61. Ferreira AJM. Analysis of composite plates using a layerwise deformation theory and multiquadrics discretization. *Mech Adv Mater Struct* 2005; 12(2): 99–112.
62. Reddy JN. *Mechanics of laminated composite plates: theory and analysis*. Boca Raton, FL: CRC Press, 1997.
63. Khdeir AA and Librescu L. Analysis of symmetric cross-ply elastic plates using a higher-order theory,part ii: buckling and free vibration. *Compos Struct* 1988; 9: 259–277.
64. Liew KM, Huang YQ and Reddy JN. Vibration analysis of symmetrically laminated plates based on fsdt using the moving least squares differential quadrature method. *Comput Meth Appl Mech Eng* 2003; 192: 2203–2222.
65. Khdeir AA and Librescu L. Analysis of symmetric cross-ply elastic plates using a higher-order theory. part ii: buckling and free vibration. *Compos Struct* 1988; 9: 259–277.
66. Liew KM and Huang YQ. Bending and buckling of thick symmetric rectangular laminates using the moving least-squeares differential quadrature method. *Int J Mech Sci* 2003; 45: 95–114.